(the scribe lines on the inside of the spherical reaction chamber are determined by this angle γ), may be expressed as

$$\sin(\gamma-\theta)=\frac{(B/R)\sin(\beta-\gamma)}{[1+(B/R)^2-2(B/R)\cos(\beta-\gamma)]^{1/2}}. \quad \text{(A1)}$$

Here B is the distance from the sphere center to the point half-way between slit edges (line BS), R is the radius of the sphere, and $\beta=21.75°$ is the polar angle of the line BS. For the target dimensions used, the denominator varied about 1/2% for $0<\gamma<90°$, so that the following relationship was used for the calculations in this paper:

$$\sin(\gamma-\theta)=0.0892\sin(\beta-\gamma). \quad \text{(A2)}$$

The location of the center of the reaction volume can be found by using the following expression for the length AS:

$$AS=B\sin(\beta-\gamma)/[\sin\gamma-(B/R)\sin\beta]. \quad \text{(A3)}$$

The path length of the N^{13} ion leaving the target holder is equal to the distance AC where

$$AC=B\sin\beta/\sin\theta+(W/2)\sin\alpha/\sin(\theta+\alpha), \quad \text{(A4)}$$

W being the slit width, i.e., the distance between slit 3 and slit 4, and $\alpha=45°$ being the angle between the exit window and the beam axis.

The path length l of the N^{13} when passing through the window is, simply,

$$l=\tau/\sin(\theta+45°), \quad \text{(A5)}$$

where τ is the window thickness.

Finally, the length L of the reaction volume along the beam axis is

$$L=W\sin\gamma/[\sin\gamma-(B/R)\sin\beta]. \quad \text{(A6)}$$

PHYSICAL REVIEW VOLUME 133, NUMBER 4B 24 FEBRUARY 1964

Cross Sections for the $Ni^{58}(\alpha,p)$, $Ni^{58}(\alpha,\gamma)$, and $Co^{59}(\alpha,n)$ Reactions

F. K. McGowan, P. H. Stelson, and W. G. Smith*
Oak Ridge National Laboratory, Oak Ridge, Tennessee
(Received 20 September 1963)

Thick-target yields have been measured for the $Ni^{58}(\alpha,\gamma)$ reaction from 4.9 to 6.1 MeV, the $Ni^{58}(\alpha,p)$ reaction from 4.9 to 11 MeV and the $Co^{59}(\alpha,n)$ reaction from 5.8 to 10 MeV. The reactions were identified by measuring the coincident annihilation radiation from the induced β^+ activities. The absolute thick-target positron yields, which were measured at approximately 100-keV energy intervals, have an accuracy of $\pm 6\%$. The reaction cross sections were obtained to an accuracy of 15 to 20% by the differentiation of the smooth thick-target yield curves. Over the measured energy range, the cross sections increase from 1 to 12 μb for the $Ni^{58}(\alpha,\gamma)$ reaction, 0.6 μb to 316 mb for the $Ni^{58}(\alpha,p)$ reaction, and 0.06 to 228 mb for the $Co^{59}(\alpha,n)$ reaction. The total reaction cross section for Ni^{58} is compared to some values predicted by optical models. The $Co^{59}(\alpha,n)$ yields are compared to those obtained by measuring the neutrons directly with the graphite sphere detector.

I. INTRODUCTION

FOR α particles with energies of 10 MeV or less, the total reaction cross section should be the sum of the following partial cross section; (α,n), (α,p), (α,γ), and (α,α'). The absolute (α,n) cross sections have been measured for a number of medium-weight targets.[1] The (α,n) threshold of 10.5 MeV for Ni^{58} is unusually high. Furthermore, at 11 MeV the (α,n) cross section is only about 1/25 of those observed for the other nickel isotopes. Presumably, therefore, the bulk of the reaction cross section for α particles with energies of 11 MeV or less on Ni^{58} must be attributed to the (α,p) reaction. Fortunately, the $Ni^{58}(\alpha,p)Cu^{61}$ reaction leads to a convenient radioactive nuclide. We have used the activation method to measure the $Ni^{58}(\alpha,p)$ cross section from $E_\alpha=4.9$ to 11 MeV.

The activation method has previously been used by Morinaga[2], and by Ball, Fairhall, and Halpern[3] to measure the $Ni^{58}(\alpha,\gamma)Zn^{62}\xrightarrow{\beta^+}Cu^{62}\xrightarrow{\beta^+}Ni^{62}$ reaction. These measurements were made for α-particle energies of about 10 MeV and higher. The observed cross sections were of the order of 100 μb. We have carried out measurements of the $Ni^{58}(\alpha,\gamma)$ cross section at the lower energies of 4.9 MeV$\leq E_\alpha \leq$6.1 MeV. At these energies the cross section varies from 1 to 10 μb. Good signal-to-noise conditions were attained by making a coincidence measurement of the annihilation γ rays following the β^+ decay.

* Deceased. Work conducted while on assignment to Oak Ridge National Laboratory as a summer research participant from Purdue University.

[1] P. H. Stelson and F. K. McGowan, following paper, Phys. Rev. 133, B911 (1964).

[2] H. Morinaga, Phys. Rev. 101, 100 (1956).

[3] J. B. Ball, A. W. Fairhall, and I. Halpern, Phys. Rev. 114, 305 (1959).

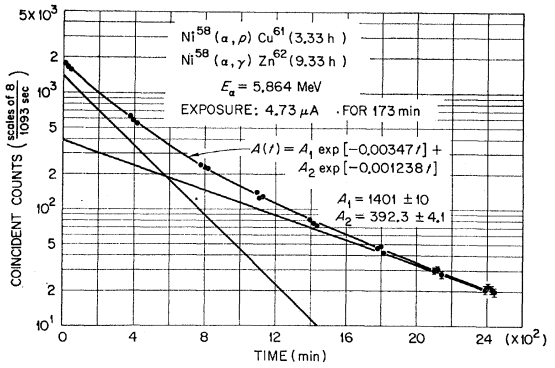

FIG. 1. Typical decay curve for the positron activity produced by α-particle bombardment of a Ni^{58} target. The decay curve has been resolved into two activities with half-lives of 3.33 and 9.33 h by a least-squares analysis.

Finally, it was thought to be worthwhile to make a comparison of an (α,n) cross section obtained by the use of the graphite sphere neutron detector and the same (α,n) cross section obtained by the activation method. The $Co^{59}(\alpha,n)Cu^{62}$ reaction was chosen for this comparison.

II. EXPERIMENTAL METHOD

Alpha particles with energies of 4 to 11 MeV were obtained from the ORNL 5.5 MV Van de Graaff. For energies up to 6 MeV, the large current resulting from acceleration of singly ionized helium was used. The small component ($\sim$0.1 μA) of doubly ionized helium was used to cover the region of 6 to 11 MeV.

Absolute thick-target yields were measured at approximately 100-keV energy intervals. Chemically pure targets of Ni^{58} enriched to 98.4% were prepared by the electrodeposition of the Ni^{58} onto 5-mil nickel backings. Targets of metallic cobalt were also prepared by electrodeposition of cobalt onto 5-mil nickel backings.

The induced β^+ activities were measured by making a coincidence count of the resulting annihilation γ rays. The target was sandwiched between two pieces of copper to stop the positrons. The annihilation γ rays were detected in two 3-$\times$3-in. NaI scintillation counters. The absolute efficiency of the system was determined to $\pm$6% by using a calibrated Na^{22} source of positrons.

III. RESULTS AND DISCUSSION

A. $Ni^{58}(\alpha,\gamma)$ and $Ni^{58}(\alpha,p)$ Reactions

The Q values for the $Ni^{58}(\alpha,\gamma)$ and $Ni^{58}(\alpha,p)$ reactions are about $+3.3$ MeV and -3.14 MeV, respectively. The threshold for the (α,p) reactions is so low that it was not possible to measure the cross section near threshold because the cross sections were too small. The lowest energy at which useful data could be obtained was E_α=4.9 MeV.

TABLE I. Summary of $Ni^{58}(\alpha,p)$ and $Ni^{58}(\alpha,\gamma)$ thick-target reaction yields and cross sections for α-particle energies of 4.9 to 6.1 MeV. Columns 2 and 4 list the thick-target yields per one μC of He^{++} particle (3.12×10^{12} incident particles). Columns 3 and 5 list the cross sections in μb.

E_α MeV	(α,p) Excitations μC	$\sigma(\alpha,p)$ (μb)	(α,γ) Excitations μC	$\sigma(\alpha,\gamma)$ (μb)
4.9	5.98	0.60	2.17×10	1.00
5.0	1.22×10	1.15	3.05×10	1.41
5.1	2.35×10	2.07	4.24×10	1.88
5.2	4.33×10	3.39	5.80×10	2.53
5.3	7.43×10	5.5	7.90×10	3.12
5.4	1.27×10^2	8.1	1.06×10^2	4.21
5.5	2.04×10^2	1.25×10	1.40×10^2	5.10
5.6	3.13×10^2	1.73×10	1.82×10^2	5.96
5.7	4.98×10^2	3.04×10	2.33×10^2	7.27
5.8	8.02×10^2	4.81×10	2.92×10^2	8.10
5.9	1.27×10^3	7.49×10	3.59×10^2	9.36
6.0	2.01×10^3	1.13×10^2	4.38×10^2	1.06×10
6.1	3.16×10^3	1.73×10^2	5.28×10^2	1.22×10

A typical decay curve for the induced β^+ activity for a Ni^{58} target is shown in Fig. 1. The target was bombarded for 172 min with 4.7 μA of 5.864-MeV α particles. The Cu^{61} produced by the $Ni^{58}(\alpha,p)$ reaction has a half-life of 3.33 h and the Zn^{62} produced by the $Ni^{58}(\alpha,\gamma)$ reaction has a half-life of 9.33 h. The observed decay curve has been decomposed by least-squares analysis into these two activities. The two decay curves are

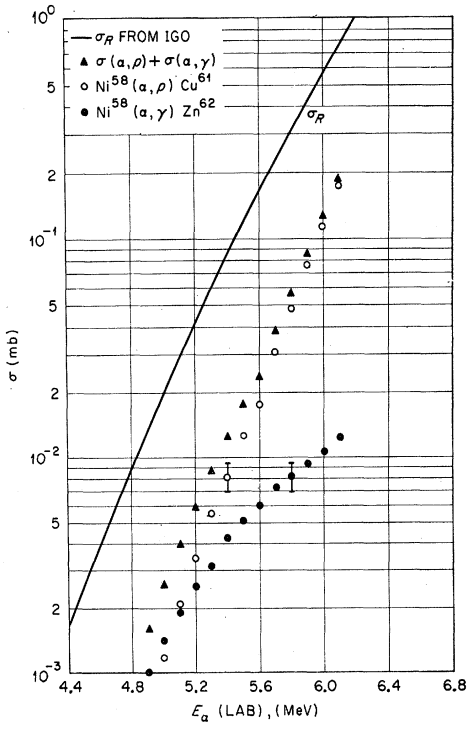

FIG. 2. The $Ni^{58}(\alpha,\gamma)$ and $Ni^{58}(\alpha,p)$ cross sections are shown for the α-particle energy range 4.9 to 6.1 MeV. The total reaction cross section which is taken as the sum of the $(\alpha,\gamma)+(\alpha,p)$ is also shown. The predicted total reaction cross section of Igo is also shown.

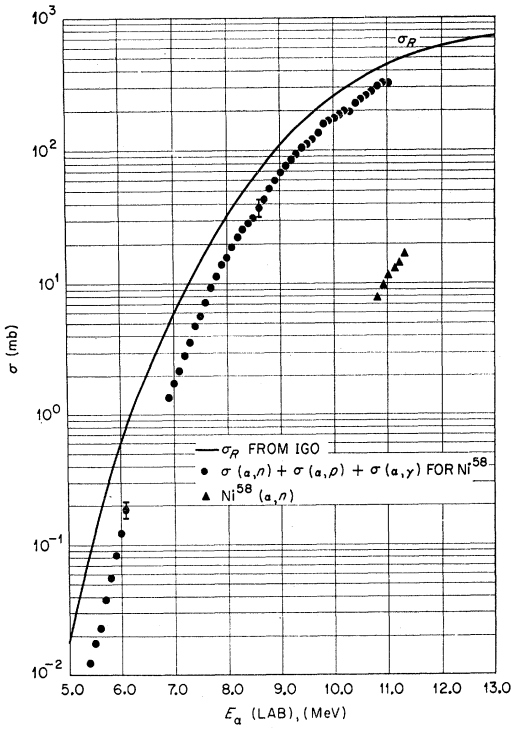

FIG. 3. The total reaction cross section for $Ni^{58}+\alpha$, which is taken as the sum of $(\alpha,p)+(\alpha,n)+(\alpha,\gamma)$ partial cross sections, is shown as a function of α-particle energy for the range 5.3 to 11 MeV. The theoretical total reaction cross section of Igo is also shown.

shown in Fig. 1. The statistical analysis showed that the observed decay was properly accounted for by the two activities with half-lives of 3.33 and 9.33 h.

Both the $Ni^{58}(\alpha,\gamma)$ and $Ni^{58}(\alpha,p)$ thick-target positron yields were measured for 4.9 MeV$<E_\alpha<$6.1 MeV. Above 6.1 MeV the yield of the (α,p) reaction became so much larger than the (α,γ) reaction that we no longer attempted to measure the (α,γ) activity. At the higher energies, sufficient Cu^{61} activity was produced with bombardment times ranging from 15 to 40 min.

In general, the thick-target positron yields have been measured to an accuracy of $\pm 6\%$. In order to get the thick-target reaction yields it is necessary to know the average number of emitted positrons per decay. For the Zn^{62} decay produced by the (α,γ) reaction we have taken 0.18 ± 0.06 β^+ per decay.[4] The Zn^{62} decays to Cu^{62} which in turn decays by β^+ activity ($T_{1/2}=9.8$ min) to stable Ni^{62}. We have taken the number of β^+ per decay of Cu^{62} as 0.98 ± 0.01.[4] Hence, the total number of β^+ particles per (α,γ) reaction is 1.16 ± 0.06. We have used this number to convert the observed number of positrons to the thick-target reaction yields. These yields for the $Ni^{58}(\alpha,\gamma)$ reaction are listed in Table I. Combining the error of our measurement and the error in the number of positrons per decay, it is estimated that the thick-target yields have an absolute accuracy of $\pm 9\%$.

The Cu^{61}, which is produced by the $Ni^{58}(\alpha,p)$ reaction, decays to several states of the Ni^{61} nucleus by positron emission and by electron capture. We have taken the number of positrons per decay as 0.61 and we estimate that this number is accurate to $\pm 15\%$.[4] Hence, the thick-target yields listed in Tables I and II for the $Ni^{58}(\alpha,p)$ reaction have an absolute accuracy of approximately $\pm 16\%$.

Cross sections were obtained by the differentiation of the measured thick-target yield curves. This method requires the knowledge of the stopping powers for α particles. It is estimated that the stopping powers are known to $\pm 8\%$. There is also an error caused by the uncertainties in differentiating the yield curve; we estimate this error as $\pm 10\%$. Combining these errors, one estimates that the $Ni^{58}(\alpha,\gamma)$ cross sections have an absolute error of $\pm 15\%$ and the $Ni^{58}(\alpha,p)$ cross sections have an absolute error of $\pm 20\%$.

The $Ni^{58}(\alpha,\gamma)$ cross sections are listed in Table I and are plotted as function of α-particle energy in Fig. 2. The cross section increases from 1 μb at 4.9 MeV to 12 μb at 6.1 MeV.

The $Ni^{58}(\alpha,p)$ cross sections are given in Table I for 4.9 MeV$<E_\alpha<$6.1 MeV and in Table II for 7.0 MeV $<E_\alpha<$11 MeV. The cross sections are plotted in Figs. 2 and 3. In the energy range 4.9 to 6.1 MeV the (α,p) reaction increases much more rapidly than the (α,γ) cross section. At 4.9 MeV the (α,p) cross section is less than the (α,γ) cross section whereas at 6.1 MeV it is about 15 times larger.

TABLE II. Summary of $Ni^{58}(\alpha,p)$ thick-target reaction yields and cross sections for α-particle energies of 7 to 11 MeV. Column 2 lists the thick-target yields per one μC of He^{++} particles (3.12×10^{12} incident particles). Column 3 lists the observed cross sections in mb.

E_α (MeV)	Excitations μC	$\sigma(\alpha,p)$ (mb)
7.0	5.66×10^4	1.74
7.2	9.47×10^4	2.79
7.4	1.59×10^5	4.78
7.6	2.62×10^5	7.26
7.8	4.28×10^5	1.15×10
8.0	6.77×10^5	1.61×10
8.2	1.03×10^6	2.24×10
8.4	1.51×10^6	2.84×10
8.6	2.10×10^6	3.74×10
8.8	2.94×10^6	5.22×10
9.0	4.11×10^6	6.98×10
9.2	5.61×10^6	8.71×10
9.4	7.50×10^6	1.07×10^2
9.6	9.77×10^6	1.22×10^2
9.8	1.26×10^7	1.61×10^2
10.0	1.60×10^7	1.74×10^2
10.2	1.97×10^7	2.03×10^2
10.4	2.41×10^7	2.32×10^2
10.6	2.92×10^7	2.61×10^2
10.8	3.52×10^7	3.04×10^2
11.0	4.17×10^7	3.16×10^2

[4] *Nuclear Data Sheets*, compiled by K. Way *et al.* (National Academy of Sciences–National Research Council, Washington, D. C., 1960).

The total reaction cross section which is taken as the sum of the $(\alpha,\gamma)+(\alpha,p)+(\alpha,n)$ is also given in Figs. 2 and 3. Igo's calculated reaction cross section is also shown in Figs. 2 and 3.[5] At 11 MeV the observed cross section is about 30% less than Igo's value. The deviation becomes progressively greater at lower α-particle energies. At $E_\alpha = 5$ to 6 MeV, the discrepancy is a factor of 5 to 10.

Bassel, Drisko, and Halbert have carried out some optical-model fits to the above Ni^{58} total reaction cross section.[6] They first tried the optical parameters which had given a good fit to the elastic scattering of 43-MeV α particles.[7] This calculation gave agreement at 11 MeV but was too large by a factor of 10 at 5 MeV. They found that by changing the depth of the imaginary well from 18.85 to 3 MeV, good agreement was obtained over the entire energy range. They point out, however, that the predicted elastic scattering angular distributions are quite different for the two cases, having an oscillatory structure at small imaginary well depths and passing to a smooth behavior at large imaginary well depths. It would be of interest to have measurements of the elastic scattering angular distribution in this lower α-particle energy region.

B. $Co^{59}(\alpha,n)Cu^{62}$ Reaction

The $Co^{59}(\alpha,n)Cu^{62}$ reaction leads to a convenient 10-min positron activity.[4] Furthermore, the (α,γ), (α,p), and (α,d) reactions, which are the other possible reactions below 10 MeV, all lead to stable nuclei. The positron decay consists of a simple, single-component exponential decay. Representative positron decay curves were measured at different α-particle energies and they all exhibited a simple exponential decay for 2 to 3 decades. Most of the positrons from the decay of Cu^{62} go to the ground state of Ni^{62}. The number of positrons per decay has little uncertainty. We have taken this number as 0.984 ± 0.010 (Ref. 4). Hence, most of the uncertainty in the determination of the absolute thick-target yield of the $Co^{59}(\alpha,n)$ reaction is caused by the detection efficiency error which is $\pm6\%$.

TABLE III. Summary of $Co^{59}(\alpha,n)$ thick-target yields and cross sections as determined by the activation method. The thick-target yields determined by the use of the graphite sphere neutron detector are also given (column 3) for comparison. The percentage difference in the yields measured by the two methods is given in column 4. Yields are for 3.12×10^{12} incident particles.

E_α (MeV)	Yield from induced activity	Yield from graphite sphere detector	% difference	σ(mb)
5.8	5.40×10^{2}	6.20×10^{2}	−13%	0.060
6.0	2.50×10^{3}	2.70×10^{3}	−8%	0.30
6.2	8.90×10^{3}	8.10×10^{3}	+9%	0.50
6.4	2.20×10^{4}	2.05×10^{4}	+7%	1.2
6.6	4.70×10^{4}	4.45×10^{4}	+8%	1.8
6.8	8.25×10^{4}	7.95×10^{4}	+4%	2.5
7.0	1.47×10^{5}	1.44×10^{5}	+2%	5.0
7.2	2.55×10^{5}	2.50×10^{5}	+2%	7.7
7.4	4.18×10^{5}	4.12×10^{5}	+1.5%	11
7.6	6.65×10^{5}	6.55×10^{5}	+1.5%	16
7.8	1.01×10^{6}	9.87×10^{5}	+2%	24
8.0	1.54×10^{6}	1.50×10^{6}	+3%	33
8.2	2.25×10^{6}	2.22×10^{6}	+1.5%	44
8.4	3.15×10^{6}	3.15×10^{6}	0%	52
8.6	4.32×10^{6}	4.38×10^{6}	−1.5%	68
8.8	5.94×10^{6}	6.05×10^{6}	−2%	95
9.0	8.04×10^{6}	8.16×10^{6}	−1.5%	124
9.2	1.04×10^{7}	1.07×10^{7}	−3%	123
9.4	1.33×10^{7}	1.38×10^{7}	−4%	153
9.6	1.66×10^{7}	1.75×10^{7}	−5%	171
9.8	2.06×10^{7}	2.17×10^{7}	−5%	189
10.0	2.56×10^{7}	2.65×10^{7}	−3%	228

The $Co^{59}(\alpha,n)$ reaction thick-target yields determined by the activation method are listed in Table III. For comparison we have also given the thick-target yields determined by the use of the graphite sphere neutron detectors.[1] Combining the errors of the two methods, one finds that the sets of yield measurements should agree to within $\pm7\%$. In the energy range 7 to 10 MeV, the average difference is 1% which is more than satisfactory. However, there is a systematic trend in the percentage differences with change in α-particle energy which is somewhat disturbing. We do not have an explanation for this trend. The cross sections derived from the activation yield measurements are also listed in Table III. The cross section is plotted as a function of α-particle energy in Fig. 6 of the paper on (α,n) yields[1] where they can be compared to the cross sections measured with the graphite sphere neutron detector.

[5] G. Igo, Phys. Rev. **115**, 1665 (1959).

[6] R. H. Bassel, R. M. Drisko, and E. C. Halbert, Electronuclear Division Annual Progress Report, ORNL-3257, p. 23, 1961 (unpublished).

[7] The optical parameters used by Bassel *et al.* to fit the elastic scattering of 43-MeV α particles on Ni^{58} were the following: (Saxon form for both real and imaginary wells); depth of real well, 45.58 MeV; depth of imaginary well, 18.85 MeV; real well radius, 6.178 F; imaginary well radius, 5.346 F; diffusivity of real well, 0.5271 F; diffusivity of imaginary well, 0.6619 F.